

# Study of MEH:PPV/AgMWCNTs Composite for Application in Schottky Diode

Anjali Yadav<sup>1, a)</sup>, Jhuma Gope<sup>1</sup>, Aditi Upadhyaya<sup>1</sup>, Saral Kumar Gupta<sup>1</sup>, Ajay Singh Verma<sup>1</sup> and Chandra Mohan Singh Negi<sup>2</sup>

<sup>1</sup>*Department of Physics, Banasthali Vidyapith, Banasthali-304022, India.*

<sup>2</sup>*Department of Electronics, Banasthali Vidyapith, Banasthali-304022, India.*

<sup>a)</sup>Corresponding author: anjaliyadav1412@gmail.com

**Abstract.** Herein, we fabricate pol [2-methoxy-5-(2-ethylhexyloxy)-1,4-phenylenevinylene] (MEH:PPV) and Silver (Ag) decorated multiwall carbon nanotubes (MWCNTs) composite based device by spin coating technique. The MWCNTs have been decorated with silver nanoparticles (NPs) via silver nitrate solution. Field emission scanning electron microscope (FESEM) results are in favor of the required conformation of Ag NPs on to the side walls of MWCNTs. The presence of Ag NPs in the composite has also been verified through X-Ray diffraction (XRD). The electrical properties of MEH:PPV/AgMWCNTs composite based devices have been analyzed to determine the various important diode parameters and to explain the charge transport mechanism in the device. The charge transport mechanism is explained by double logarithmic I-V curve, which show two distinct mechanisms: Ohmic conduction at low voltage and trap limited space charge conduction (TCLC) at large applied voltages.

## INTRODUCTION

Since the breakthrough discovery of carbon nanotubes (CNTs) by Ijima in 1991 [1, 2], they have been proved to be an excellent candidate for many potential applications due to their high aspect ratio, exceptional electrical properties, tensile strength, and mechanical properties [3,4]. However, in the case of CNTs it is rather difficult to achieve an appropriate dispersion and strong interfacial interactions with other material systems [5]. This insolubility problem can be alleviated through the functionalization of CNTs, since it prevents the aggregation, thus improves dispersion into solvents by the surface modifications of CNTs. In addition, it is very essential to increase the electrical conductivity of CNT based devices in order to achieve the desired performance. Decoration of the external surface of CNTs with metal nanoparticles (NPs) is a familiar method to improve the performance of the resulting device [6]. Due to large electrical conductivity of Ag NPs, decoration of MWCNTs with Ag NPs is therefore shown to be more prominent among all other metal NPs for improving the electrical conductivity of CNTs [7].

On the other hand, conjugated polymers and their derivatives have been drawing huge attention for application in electronic and optoelectronic devices due to their favorable properties such as ease of fabrication, flexibility, low cost and light weight than inorganic based devices [8,9]. Poly[2-methoxy-5-(2-ethylhexyloxy)-1,4-phenylenevinylene] (MEH:PPV) is an attractive polymer material, which is widely used in various organic devices, such as organic light emitting diodes (LED), organic solar cells, and organic photodetectors [10]. It has been generally used as donor material in the production of bulk heterojunction photovoltaic devices.

In the present manuscript, we have attached the Ag NPs onto the side walls of MWCNTs. XRD and FESEM techniques have been used to confirm the decorated AgMWCNTs. MEH:PPV and MEH:PPV/AgMWCNTs composite based devices have been characterized using current-voltage (I-V) measurements. The Analysis of I-V curves provide useful information about the diode parameters and charge transport mechanisms. It also allow to investigate the effect of inclusion of AgMWCNTs in MEH:PPV based device.

## EXPERIMENTAL DETAILS

The side walls of MWCNTs have been decorated via silver nitrate solution. The MEH:PPV/AgMWCNTs composite has been prepared using the magnetic stirring technique. For fabrication of device based on the prepared MEH:PPV/AgMWCNTs composite, we initially deposit PEDOT:PSS over the cleaned Indium Tin Oxide (ITO) coated glass substrate. A layer of MEH:PPV/AgMWCNTs composite has been applied above the PEDOT:PSS layer. All the depositions have been carried out in  $N_2$  atmosphere inside the glove Box. Back-contact of Aluminum (Al) has thermally been evaporated over the topmost layer. Dispersion of AgMWCNTs has been studied using field emission scanning electron microscope (FESEM). The electrical measurement of the fabricated devices has been obtained by the 2612A Keithley source meter attached with a manual probe station. The schematic diagram of device structure along with its corresponding energy level diagram is shown in Fig. 1.

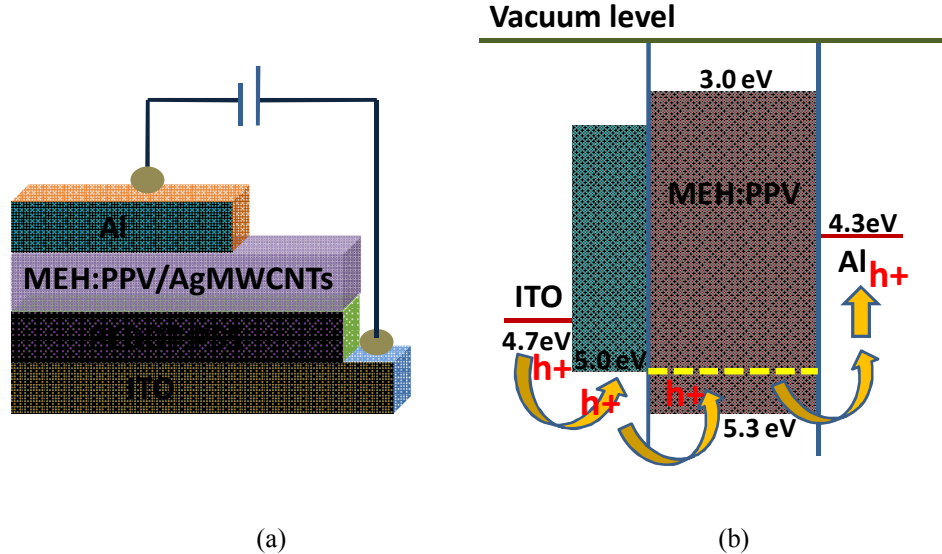


FIGURE 1. (a) Schematic diagram of device structure, (b) corresponding energy level diagram.

## RESULTS AND DISCUSSION

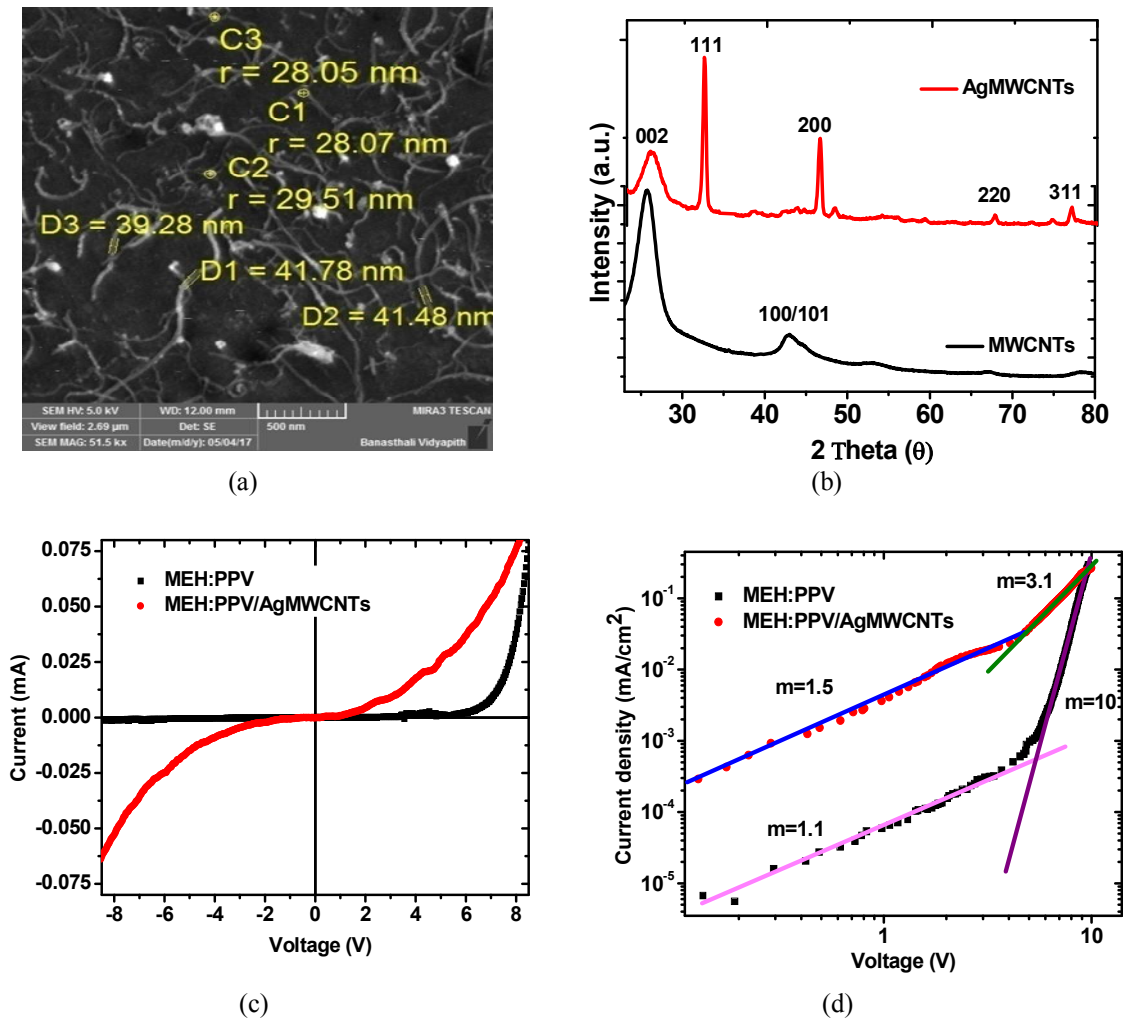
The FESEM image showing dispersion of AgMWCNT is depicted in Fig. 2(a). It is clearly observable that all the MWCNTs are uniformly distributed over the entire surface. This also confirms the attachment of the Ag NPs on the side walls of MWCNTs. As can be seen in the Fig. 2 (a), the average size of Ag NPs is around 30nm, whereas, the average diameter of AgMWCNTs is approximately 41 nm.

Figure. 2 (b), shows the XRD patterns of pristine MWCNTs and AgMWCNTs. The pristine MWCNTs exhibit reflection peaks at  $26^\circ$  and  $43^\circ$ , corresponding to (002) and (100)/(101) planes, respectively [11]. The Ag decorated MWCNTs demonstrates four individual diffraction peaks at  $34.5^\circ$ ,  $46^\circ$ ,  $67^\circ$  and  $77.5^\circ$  corresponding to the (111), (200), (220) and (311) planes of Ag, respectively, as well as peak at  $26^\circ$  related to the (002) planes of MWCNTs. The FESEM and XRD analysis clearly indicates successful decoration of MWCNTs by Ag.

Next we evaluate the performance of pristine MEH:PPV and MEH:PPV/AgMWCNTs nanocomposite based devices through I-V measurements. Figure. 2 (c) presents the comparative I-V characteristics of pristine MEH:PPV and MEH:PPV/AgMWCNTs nanocomposite based devices in dark. Both the devices show exponential dependence of current on forward voltage. For reverse applied voltages, pristine device show negligible constant current, while for MEH:PPV/AgMWCNTs nanocomposite based device, negligible constant current is observed only upto  $-3V$ , beyond that current increases rapidly with the applied voltage. This indicates devices exhibit rectification behavior due to the formation of Schottky barrier at MEH:PPV/Al interface. As can be understood from the energy band diagram shown in Fig. 1(b), when device is forward biased, the hole can be easily injected from ITO to the polymer layer through PEDOT:PSS owing to the small barrier and then transported towards Al interface from where they can be transported to the Al by thermionic emission. For reverse applied voltages, The hole faces a large barrier of  $\sim 1.1$  eV at MEH:PPV/Al interface, which further increases with increase in the reverse applied voltage, thus holes are

incapable in crossing the barrier, that might be the reason of the negligible current flow under reverse applied voltage. By replacing the MEH:PPV with the MEH:PPV/AgMWCNTs in the active layer we found the dramatic increases in the forward current and reduction in the turn on voltage. The improvement in the forward characteristics is attributed to the increase in the conductivity, and lowering of the injection barrier for holes by addition of AgMWCNTs in MEH:PPV, as indicated by the dotted yellow line in Fig. 1 (b). The conductivity increases because MWCNTs provides appropriate path for charge transport and highly conductive Ag NPs further enhances the transport of charge carriers.

Afterward, we estimate the diode parameters with the help of cheung-cheung approach [12]. The extracted diode parameters are listed in Table 1. We found that MEH:PPV/AgMWCNTs nanocomposite based device exhibit relatively better diode parameters compared to the pristine device. The reduction in barrier height and series resistance for composite based device leads to the better charge extraction which consecutively enhances the current values for composite based device, which is also reflected in the dark I-V curves as shown in Fig. 1(c). The quality of the interface, surface and thin film can also be anticipated by the value of ideality factor. We have found the ideality factor deviated from 1 for both the devices which is due to many reasons, such as, the irregularities in the thickness of organic film, uneven interfaces, large series resistance; and increased recombination due to traps and impurities [13].



**FIGURE 1.** (a) FESEM image of dispersed Ag decorated MWCNTs, (b) XRD patterns of; pristine MWCNTs and AgMWCNTs (c) comparative I-V characteristics of pristine MEH:PPV and MEH:PPV/AgMWCNTs composite based device and (d) double logarithmic J-V plot for both MEH:PPV and MEH:PPV/AgMWCNTs composite based devices.

These factors influence the performance of the device in various ways, like, the irregularities in the thickness of film indicates that transport mechanism is not dominated by the thermionic emission of the charge carriers, the uneven interfaces of the device leads to dominance of recombination current. Moreover, the series resistance occurs due to the internal losses and because of the bad contacts. The larger separation between the electrodes of the cell also affects the series resistance of the device. Lesser ideality factor of the composite based device indicates better interface and good contact between the metal and the composite layer.

**TABLE 1.** estimated diode parameters for ITO/PEDOT:PSS/MEH:PPV/AgMWCNTs/Al device.

S. No.	Device (active layer)	Reverse saturation current ( $I_s$ ) (A)	Barrier height ( $\phi_b$ ) (V)	Ideality factor (n)	Series resistance ( $R_s$ ) ( $\Omega$ )
1.	MEH:PPV	$9.7 \times 10^{-5}$	0.876	9.2	706.92
2.	MEH:PPV/AgMWCNTs	$1.3 \times 10^{-4}$	0.869	7.9	410.01

For elucidating the charge transport mechanism of the devices, we present the current density-voltage curves on double log scale in Fig. 2 (d). The value of slope,  $m \sim 1$  for low voltage range indicates is current conduction follows the ohmic behavior. At this voltage range the injection of the charge carriers by the electrodes is less, therefore thermally generated charge carriers presented in the active layer is drifted by the external applied forward voltage and give rise to the ohmic current. Thereafter, the curves start to change the behavior as the applied voltage increased to the value after that the injection carriers dominate the transport process. The current conduction is now governed by the space charge limited conduction (SCLC) under the presence of distributed traps within the forbidden gap, as indicated by the slope  $m > 2$  in Fig.2 (d).

## CONCLUSIONS

In this work, we have decorated MWCNTs with the Ag NPs. The decoration of Ag-MWCNTs has been confirmed using FESEM and XRD. We further prepare MEH:PPV/AgMWCNTs composite device and investigated its electrical properties. The incorporation of Ag-MWCNTs in MEH:PPV improves the forward voltage characteristics than pristine based device. The composite based device reveals better diode parameters, which is also reflected in the corresponding I-V curves. The charge transport mechanism investigated using double logarithmic J-V curves indicate that the conduction is first governed by the ohmic conduction in the low voltage range, and then followed by the SCLC in the high voltage region. Overall, these results help in fundamental understanding towards development of MEH:PPV/AgMWCNTs composites based optoelectronic and photovoltaic devices.

## ACKNOWLEDGMENTS

The authors gratefully acknowledge financial support from DST, India under CURIE program (grant No. SR/CURIE- Phase-III/01/2015(G)) and MHRD FAST Programme (grant No.5-5/2014-TS.VII), Govt. of India.

## REFERENCES

1. J. Prasek, J. Drbohlavova, J. Chomoucka, J. Hubalek, O. Jasek, V. Adam, R. Kizek, J. Mater. Chem. **21**, 15872 (2011).
2. S. Iijima, Nature. **354**, 56 (1991).
3. C.-X. Liu, J.-W. Choi. **2**, 329 (2012).
4. T.T. Nguyen, S.U. Nguyen, D.T. Phuong, D.C. Nguyen, A.T. Mai, Adv. Nat. Sci. Nanosci. Nanotechnol. **2**, 35015(2011).
5. B. Li, L. Li, B. Wang, C.Y. Li, Nat. Nanotechnol. **4**, 358(2009).
6. M. Shahi, S. Gautam, P. V. Shah, J.S. Rawat, P.K. Chaudhury, Harsh, R.P. Tandon, J. Nanoparticle Res. **15**, 1497(2013).

7. S. Guo, S. Dong, *TrAC Trends Anal. Chem.* **28**, 96(2009).
8. A.K. Singh, R. Prakash, *RSC Adv.* **2**, 5277(2012).
9. N. Diouri, M. Baitoul, M. Maaza, *J. Nanomater.* **2013**, 1(2013).
10. K. Kim, J.W. Shin, Y.B. Lee, M.Y. Cho, S.H. Lee, D.H. Park, D.K. Jang, C.J. Lee, J. Joo, *ACS Nano.* **4**, 4197(2010).
11. Y. Peng, Q. Chen., *Nanoscale Res. Lett.* **7**, 195(2012).
12. A. Yadav, A. Upadhyaya, S.K. Gupta, A.S. Verma, C.M.S. Negi, *Superlattices & Microstruct.*, **120**, 788 (2018).
13. A. Yadav, A. Upadhyaya, S.K. Gupta, A.S. Verma, A. Singh, P. Rathore and C.M.S. Negi, *J. Mater. Sci. Mater. Electron.* **29**, 7979(2018).